Density-functional theory based calculations of spin-orbit interaction in ZnO

メタデータ	言語: eng
	出版者:
	公開日: 2017-10-05
	キーワード (Ja):
	キーワード (En):
	作成者:
	メールアドレス:
	所属:
URL	http://hdl.handle.net/2297/43818

Abstract for Dissertation

Density-Functional Theory Based Calculations of Spin-Orbit Interaction in ZnO

ZnO におけるスピン軌道相互作用の密度汎関数理論に基づく計算

MOH. ADHIB ULIL ABSOR

1223102008

Graduate School of Natural Science and Technology

Division of Mathematical and Physical Sciences

Kanazawa University

July 2015

I. Introduction

Recently, the field of spintronics attracted much scientific interest because of their potential applications in future electronic devices [1,2]. The spintronics or spin electronics refers to the study of the physical properties of electron spin in solid state physics, and related to the possible devices by exploiting spin in addition to charge degree of freedom. One of the important discovery of spintronics is giant magnetoresistance (GMR), which is observed in metallic multilayers by using a spin-dependent electron transport measurement [3,4]. Furthermore, the next generation of the spintronics is focused on the semiconductor class, such as dilute magnetic semiconductors (DMS), which has been extensively studied [5,6]. Here, some of important novel physical properties which are useful for spintronics such as carrier-induced ferromagnetism and photoinduced ferromagnetism were found [7,8].

Thus far, recent development of spintronics relies on the new pathway for exploiting carrier spins in semiconductors without any addition of magnetic materials or external magnetic fields, which can be realized by incorporating the spin orbit interactions (SOI) [9,10]. This approach becomes an alternative way since SOI enables the generation and manipulation of spin solely by electric fields or strain effect. Especially, the Rashba effect [9] attracted much attention because it plays an important role in the spintronics device operation such as the spin-field effect transistor (SFET) [10]. On the other hand, current-induced spin polarization [11] and spin Hall effect [12] are the important of example fundamental phenomena in spintronics where the SOI has a crucial contribution.

Recently, a new spintronics system based SOI known as persistent spin helix (PSH) attracted much scientific attention [13-20]. In this system, the strongly enhanced spin lifetime has been experimentally observed, which opens a new gateway to realize an efficient spintronics devices.

For the spintronics based SOI, two dimensional electron gas (2DEG) system is an ideal platform for spintronics since it can be effectively controlled by using the external electric field or by strain effect. In this case, ZnO is promising since the high quality of the 2DEG has been experimentally observed. Here, the quantum Hall effect [21] and the fractional quantum Hall effect [22] has been experimentally observed. The high carrier concentrations (up to 10^{13} cm^{-2}) and the high mobility (larger than 10^5 cm^2.V^{-1}.s^{-1}) at low temperature have been reported [22]. Furthermore, the fabrication of the 2DEG in samples grown with metalorganic vapor deposition has been conducted, which is suitable for mass production [23]. Therefore, the application of ZnO as a spintronics material is plausible, which is supported by the fact that the spin polarization of the 2DEG [24] and the long spin lifetime [25] of ZnO interface have been experimentally observed.

Since ZnO is promising for spintronics applications as mentioned above, the study of SOI is crucially important. In this dissertation, the effect of the SOI on ZnO has been studied by using density functional theory (DFT) implemented on the OpenMX code [26]. We evaluate the spin structures to analyse the physical properties induced by SOI. Here, two different cases have been considered: (i) the strained bulk system and (ii) the surface system oriented on the [10-10] direction.

II. Some of Important Results and Discussion

A. Tunable Rashba effect on strained ZnO

The first part of this dissertation is to investigate the effect of SOI on strained ZnO. In the most stable phases, ZnO forms wurtzite structure in which the unit vectors of the unit cell are given by $a_1=(1/2,3^{1/2}/2,0)a$, $a_2=(1/2,-3^{1/2}/2,0)a$, and $a_3=(00,c/a)a$, where a and c are the lattice constant in the a- and c-directions, respectively [see insert Fig. 1(b)]. The Zn atoms are located at $(0,0,0)$ and $(2/3,1/3,1/2)$ whereas the O atoms are located on $(0,0,u)$ and $(2/3, 1/3,1/2+u)$. The length of Zn-O bond along c-axis is givn by $d = uc$, where u is the internal parameter.
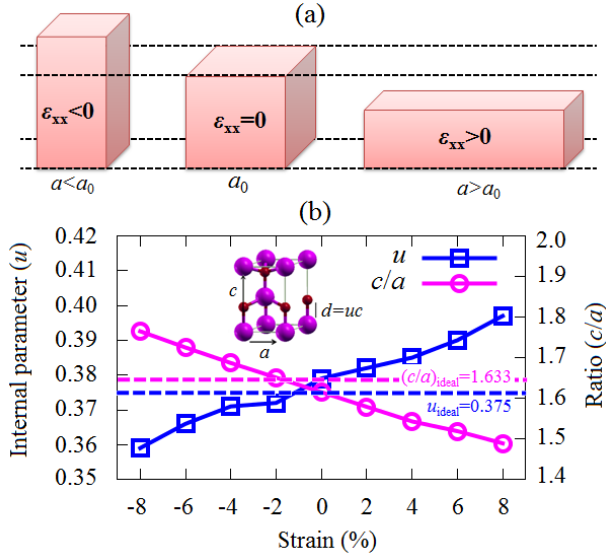

Figure 1. (a) The effect of strain on the bulk ZnO. Two different cases are considered that are the tensile biaxial strain (right side) and compressive biaxial strain (left side). (b) The calculated result of the optimize structural parameter as a function of strain. The insert shows the unit cell of wurtzite ZnO.

We consider a wide range of biaxial strain (up to $\pm 8\%$) which is perpendicular to the c axis. We study two different cases, i.e, the tensile biaxial strain (TBS) which increases the in-plane lattice constant a and the compressive biaxial strain (CBS) which decreases a [Figures 1 (a)]. The calculated result of the optimized structural parameter is shown in Fig. 1(b). We find that the value of c/a ratio decreases (increases) under the TBS (CBS), whereas the internal parameter u increases (decreases) under TBS (CBS). Therefore, we clarify that the structural parameter is sensitively affected by the strain, which is expected to induce new physical properties for spintronics.

We then investigate the effect of the SOI on strained ZnO. We focused on the SOI on the conduction band minimum (CBM) since n-type ZnO is achieved by introducing Mg doping [27]. As shown in Fig. 2, for the case of unstrained system, very small spin-split bands are identified, which are degenerated at the Γ point because of time reversibility. In these spin-split bands, we find anti-clockwise and clockwise orientation of the Rashba spin rotation for the upper and lower band, respectively. When we introduce biaxial strain, the band splitting substantially enhances. In the case

of TBS, the Rashba spin rotations are similar to those of the unstrained system. On the contrary, the direction of Rashba spin rotations becomes opposite in the case of CBS, indicating that the Rashba spin rotations can be inversed by applying biaxial strain.
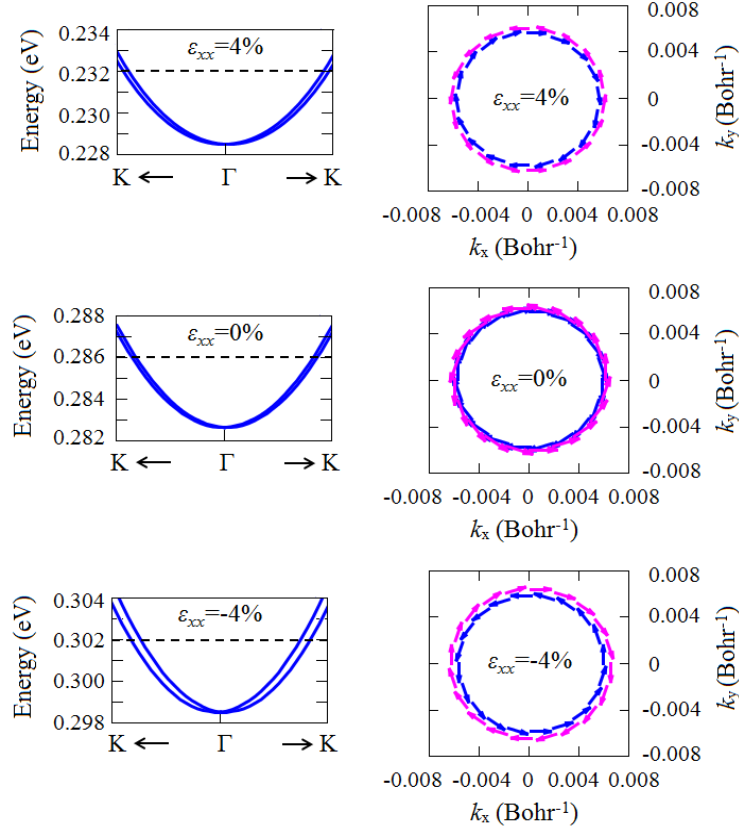

Figure 2. The spin-split band and spin textures under strain effect. The spin textures are calculated on 3.5 meV above the degenerate state of at CBB

To understand the origin of the inversion of the Rashba spin rotation, we consider the SOI Hamiltonian of the two dimensional free electron system which is expressed as $H_{SOI}=\alpha_R(k_y\sigma_x-k_x\sigma_y)$, where k_x and k_y are the wave vectors in the x- and y-directions, respectively, and σ_x and σ_y are Pauli matrixes. In this expression, α_R is the Rashba spin-orbit strength which is defined as $\alpha_R=-e\hbar E_z/4m^2c^2$, where E_z, m, c, and e are the electric field in the z-directions, the effective mass, the light velocity, and the elementary charge respectively. When $E_z>0$, this leads to the fact that the condition of $\alpha_R>0$ is obtained. Therefore, the Rashba spin-rotation are clockwise and anti-clockwise direction for the upper and lower band respectively. On the contrary, opposite Rashba spin rotations are achieved when $E_z>0$ since it leads to the case of $\alpha_R<0$.

Considering the above arguments and our calculation results of the Rashba spin rotation in Fig. 2, we expect that the negative and positive electric fields E_z are introduced under the CBS and TBS, respectively. These signs of the electric field are consistent with those calculated by using a simple point charge model (PCM) as discussed hereafter. We here consider the PCM including Zn^{2+} and O^{2-} ions as shown in Fig. 3(a). We evaluate the polarization difference defined as

$\Delta P = P(c/a, u) - P(c/a, u_{ideal})$, where c/a and u are optimized for a given biaxial strain and $u_{ideal} = 0.375$. Under substantial CBS, $u < u_{ideal}$ [Fig. 3(a)]. Therefore, the PCM leads to the positive ΔP [Fig.3(b)]. This positive value of ΔP is expected to induce the fact that $E_z > 0$. On the contrary, substantial TBS leads to the fact that $u > u_{ideal}$. As a result, the negative ΔP and positive E_z are induced. We therefore conclude that the negative and positive E_z are introduced under CBS and TBS, respectively, and that the directions of the Rashba spin rotations in Fig. 2 are well-explained based on the PCM.
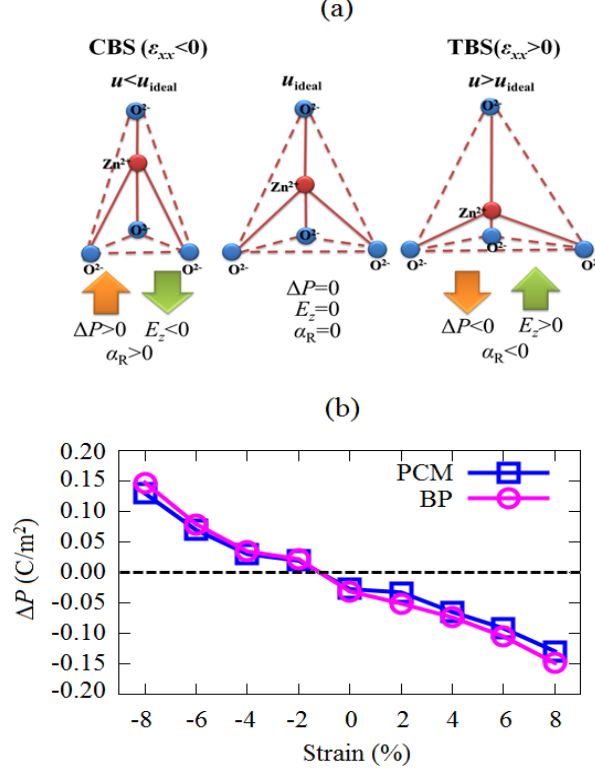

Figure 3. (a) Relation between structural parameter and Rashba spin-orbit strength. (b) The calculated data of the electric polarization different as a function of strain calculated by the PCM and BP methods

To confirm the reliability of the above-mentioned PCM, we here calculate the electric polarization by using Berry phase (BP) method [28,29] [Fig. 3(b)]. In the case of the unstrained system, the value of ΔP calculated from the BP method is -0.031 C/m^2, which is very close to the result obtained by using the PCM (-0.0271 C/m^2). These values are close to those of past calculations (-0.032 to -0.057 C/m^2) [30-31]. When we introduce biaxial strain, we find that our results of ΔP calculated from the PCM are close to those calculated from the BP method, which indicates that the PCM is reliable [Fig. 3(b)].

Here, we present the calculated results of the Rashba spin-orbit strength α_R, which is useful for spintronics devices applications. As shown in Fig. 4 that the absolute values of Rashba spin-orbit strength α_R enhances under increasing of strain. This indicates that the values of α_R can be effectively controlled by tuning the strain. This strain can be achieved by using impurity doping [32] and/or

introducing lattice mismatch between ZnO and substrate [33]. Then, our findings of the tunable Rashba effect by applying the biaxial strain are useful to realize spintronics applications of ZnO.
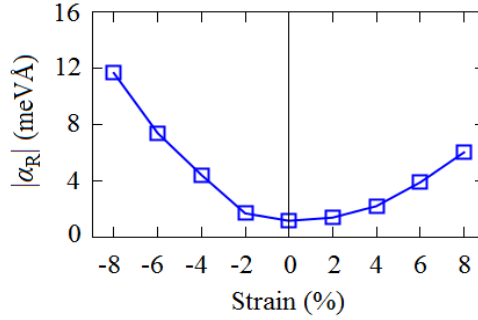

Figure 4. The absolute values of the Rashba spin-orbit strength as a function of strain.

Recently, the quantum well structure of ZnO has been extensively studied [34,35]. Our calculations indicate that two quantum wells consisting of n-type ZnO having opposite directions of the Rashba spin rotations can be realized. By using two quantum wells separated by an energy barrier, an effective spin-filtering due to tunneling is expected to be achieved. In fact, for the spin-filtering device proposed by Koga et. al, two quantum wells having the opposite directions of the Rashba spin rotations were used [36]. Their proposal may give some hint for the device applications of the reversible Rashba effect on ZnO.

Finally, we discuss another possible application of strained ZnO. We find that the Rashba splitting of the unstrained system is small [the absolute values of α_R=1.15 meVÅ], which is consistent with the observed long spin relaxation time [37]. In fact, a very small Rashba effect on MgZnO/ZnO interface [α_R=0.70 meVÅ] has been experimentally observed [38]. It is expected that the zero (or very small) Rashba splitting can be achieved when we introduce suitable small biaxial strain. When the Rashba effect on ZnO is extremely small, we can achieve a very long spin coherence. Then, ZnO can be used as an efficient spintronics devices.

B. Persistent spin helix on ZnO(10-10) surface

The second part of this dissertation is to study the effect of SOI on the surface system. Here, we consider a surface system oriented on the [10-10] direction. The crystal geometric of the surface and its Brillouin zone are shown in Fig. 5 (a) and (b). Our calculation revealed that occupied surface states appear in band structures in the energy range of -1.3 to -0.65 eV [Fig. 5(c)]. We calculate the partial density of states (PDOS) projected onto the surface atoms [Fig. 5(d)] and find that that the occupied surface state is characterized by O-2p orbitals, which is consistent with the results of past calculations [39]. Given that the surface states are occupied, doping is expected to create a p-type system. Indeed, several studies have succeeded in producing p-type, non-polar wurtzite ZnO films [40,41], giving credence to the notion of creating a p-type wurtzite ZnO(10-10) surface.

The effect of SOC on the surface states can be seen in Fig. 6, wherein the band splitting is small in the Γ-Y direction, but quite large in the Γ-X direction. In these pin-split surface state bands,

we find that the spin textures exhibit a quasi-one-dimensional orientation in the inplane y-direction [Fig. 7(a)], yet also have out-of-plane z- components [Fig. 7(b)]. These quasi-one dimensional spin textures are expected to generate current in a direction perpendicular to the spin orientation, as well as induce a greatly enhanced spin relaxation time through the PSH mechanism[13]. This is supported by the fact that a similar PSH has been observed in [110]-oriented zinc-blende QWs with out-of-plane spin orientations [20].
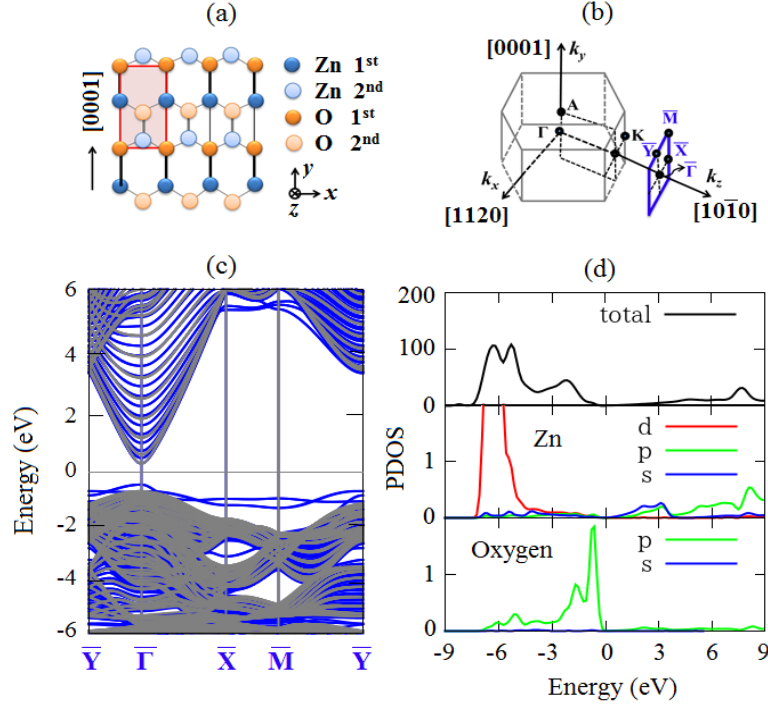

Figure 5. (a) Top view of the crystal geometry of ZnO (10-10) surface. (b) Surface Brillouin zone. (c) Band structure of ZnO(10-10) surface. The blue and black lines correspond to the band structures of surface and bulk system, respectively. (d) Total and partial density of states projected onto the surface atoms.

To better understand the origin of spin textures, we must consider the SOI of surface states based on group theory[42-44]. This states that the ZnO(10-10) surface belongs to the symmetry point group C_s: the mirror reflections in operation in this symmetry transforms (x,y,z) to $(-x,y,z)$. Considering the fact that the SOI Hamiltonian is totally symmetric in the C_s point group and includes first-order terms over the wave vectors, SOC can be expressed as $H_{SOI}=\alpha_1 k_x \sigma_z + \alpha_2 k_x \sigma_y + \alpha_3 k_y \sigma_x$, where α_1, α_2, and α_3 are the spin-orbit strengths. Here, α_1 is characterized by the in-plane electric field E_y, whereas α_2 and α_3 relate to the out-of-plane electric field E_z that originates from the surface effect.

In the case of a bulk system oriented in the [10-10] direction, the out-of-plane electric field E_z vanishes. Consequently, in the $k_x - k_y$ plane, both α_2 and α_3 are zero. This leads to a case in which only the first term of H_{SOI} in Eq. (4) remains, meaning that the bands are spin degenerated in the Γ-Y direction and the spin textures are oriented to the out-of-plane z-direction. In surface states, on the other hand, a band split is introduced in the Γ-Y direction due to the third term of H_{SOI} in Eq. (4) [Fig.

6]. Furthermore, as a result of the second term in this equation, a tilting of the spin textures in the in-plane *y*-direction is induced [Fig. 7]. It can therefore be concluded that the above spin-orbit Hamiltonian of the surface state matches well with the calculated results, i.e., the band split in the Γ-*Y* direction and the tilt of the spin textures.
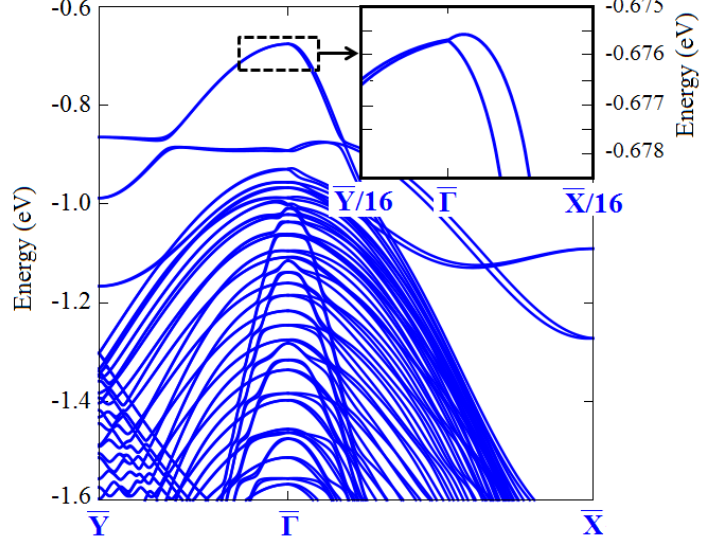

Figure 6. The spin-split states bands at valence band maximum. The insert shows the spin-split band of the surface states.
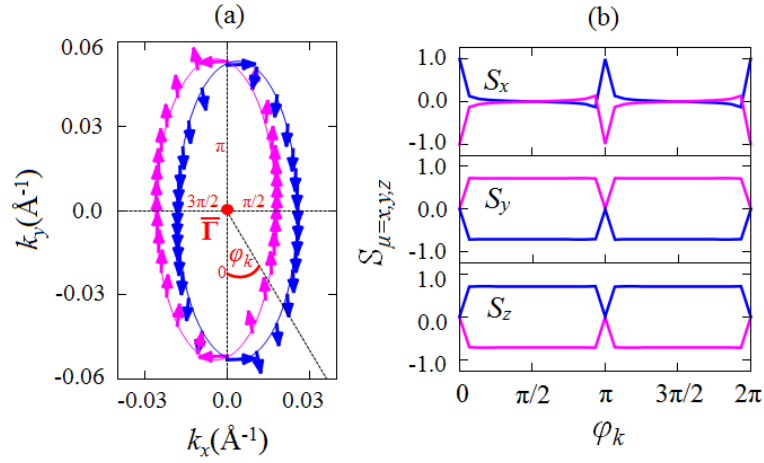

Figure 7. (a) The spin textures of the surface state at VBM. The band energy of the spin textures is 1 meV below the highest energy in the occupied surface state. The arrows represent the spin directions projected to the k_x-k_y plane. (b) Relationships between rotation angle (φ_k) and spin components.

Since H_{SOI} is strongly affected by the electric field as mentioned above, the origin of the spin textures can be further clarified by studying the electric polarization. On the basis that the spin-split surface state is strongly localized in the first two-bilayers [Fig. 8(a)], the strong electric polarization is expected to occure in these bilayers. To clarify this, the layer-dependence of the electric polarization

was calculated using a point charge model (PCM). As shown in Fig. 8(b), this reveals that the strongest electric polarization is identified near the first bilayer.

Electric polarization in the out-of-plane ΔP_z and in-plane ΔP_y directions was calculated to be 0.077 C/m^2 and -0.081 C/m^2, respectively. These values indicate that the electric field in the out-of-plane E_z direction is comparable to that in the in-plane E_y direction, which would induce a tilting of the spin orientation [Fig. 8(c)]. However, only the in-plane electric polarization is observed in the case of bulk system [$\Delta P_{y\text{-bulk}}$= -0.027 C/m^2]. This leads to the fact that the in-plane elctric field E_y is generated, but induces a spin orientation with a fully out-of-plane z-direction [Fig. 8(d)]. This would confirm that the spin textures in Fig. 7 are well-consistent with the PCM results.
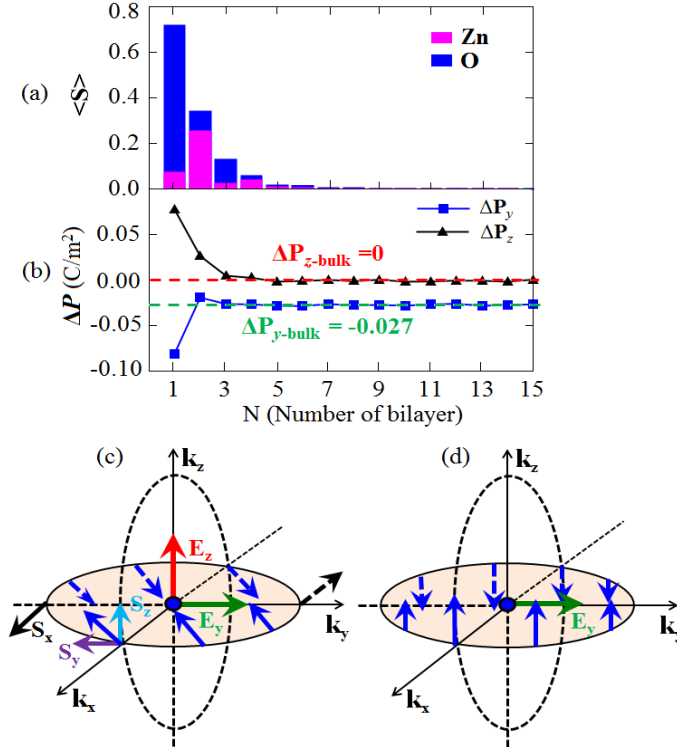

Figure 8. (a) Expected values of spin projected to the atoms in each bilayers. The calculations are performed in the surface state in Fig. 7(a). The top of the surface is represented by N=1. (b) Calculated data on the in-plane and out-of-plane electric polarizations in each bilayers using PCM. Schematic view of the spin textures and electric fields for the case of the surface (c) and bulk systems (d).

Recently, PSH that induces a greatly enhanced spin relaxation time has been extensively studied [13-20], with our calculations indicating that this is in fact achieved using the ZnO(10-10) surface. Since the calculated results of spin textures show a quasi-one-dimensional orientation, this inhibits the precession of the spins, thereby increasing the spin relaxation time. A similar mechanism behind long spin relaxation times has been reported in [110]-oriented zinc-blende QWs [45-47], suggesting that the ZnO(10-10) surface could provide an efficient spintronics device.

The spin-orbit strength of the PSH (α_{PSH}), a variable of interest in spintronics device applications, was calculated using the band dispersion in Fig. 2. This found that the value of α_{PSH} is

quite substantial (34.78 meVÅ) and much larger than what has been observed in the PSH of various zinc-blende n-type QW structures of GaAs/AlGaAs [3.5 to 4.9 meVÅ) [15], 2.77 meVÅ [19]] and InAlAs/InGaAs [1.0 meVÅ [17], 2.0 meV°A [18]]. This large value of α_{PSH} should ensure a small wavelength of PSH (λ_{PSH}), which is important to the miniaturization of spintronics devices. As it happens, the calculated value λ_{PSH} (0.19 μm) was in fact one-order less than that observed in the direct mapping of PSH (7.3 to 10 μm [15]) and the resonant inelastic light-scattering measurement (5.5 μm [19]) of GaAs/AlGaAs QWs.

III. Conclussion

We have systematically studied the effect of SOI on ZnO by using first-principles DFT calculations. For the case of the strained bulk system, we revealed that the SOI shows the Rashba type. We found that the Rashba spin rotation can be inversed by applying biaxial strain. Furthermore, we revealed that the Rashba spin-orbit strength can be effectively controlled by tuning the strain, suggesting that the strained bulk system   is suitable for spintronics applications.

In the case of surface system, on the other hand, we found that the SOI leads to the persistent spin helix (PSH), exhibiting a quasi-one dimensional orientation of the spin textures. This particular of PSH is expected to induce the long spin lifetime, which is important to realize energy-saving spintronics devices. Furthermore, we revealed that the wavelength of this PSH is smaller than that observed with various zinc-blende quantum well structures, suggesting that the present system enables for the miniaturization of the spintronics devices.

Finally, we conclude that both the strained bulk and the surface system are promising for spintronics applications.

Bibliography

[1] I. Zutic, J. Fabian, and S. D. Sarma, Rev. Mod. Phys. **76**, 323 (2004).

[2] A. Hirohata and K. Takanashi, J. Ohys. D, Apl. Phys. **47**, 193001 (2014).

[3] M. N. Baibich et. al., Phys. Rev. Lett. **61**, 2472 (1988).

[4] G. Binasch et. al., Phys. Rev. B **39**, 4828 (1989).

[5] R. Fiederling et. al., Nature **402**, 787 (1999).

[6] H. Ohno et. al., Nature **408**, 944 (2000).

[7] M. Tanaka and Y. Higo, Phys. Rev. Lett. **87**, 026602 (2001).

[8] S. Mishra, G. S. Tripathi, and S. Satpathi, Phys. Rev. B **77**, 125216 (2008).

[9] Y. A. Bychkov and E. I. Rashba: J. Phys. C **17,** 6039 (1984).

[10] S. Datta and B. Das: Appl. Phys. Lett. **56,** 665 (1990).

[11] S. Kuhlen, et. al., Phys. Rev. Lett. **109**, 146603 (2012).

[12] X.-L. Qi, Y.-S. Wu, and S.-C. Zhang, Phys. Rev. B **74**, 085308 (2006).

[13] B. A. Bernevig, J. Orenstein, and S.-C. Zhang, Phys. Rev. Lett. **97**, 236601 (2006).

[14] J. D. Koralek, et. al., Nature **458**, 610 (2009).

[15] M. P. Walser, C. Reichl, W. Wegscheider, and G. Salis, Nat. Phys. **8**, 757 (2012).

[16] M. Kohda, et. al., Phys. Rev. B **86**, 081306 (2012).

[17] J. Ishihara, Y. Ohno, and H. Ohno, Applied Physics Express **7**, 013001 (2014).

[18] A. Sasaki, et. al., Nat. Nano. **9**, 703 (2014).

[19] C. Schonhuber, et. al., Phys. Rev. B **89**, 085406 (2014).

[20] Y. S. Chen, S. Falt, W. Wegscheider, and G. Salis, Phys. Rev. B **90**, 121304(2014).

[21] A. Tsukazaki, et. al., Science **315,** 1388 (2007).

[22] A. Tsukazaki, et. al., Nat. Mater. **9,** 889 (2010).

[23] J. Ye et. al., Sci. Rep. **2**, 533, (2012).

[24] K. Han, et. al., Appl. Phys. Lett. **100**, 192105 (2012).

[25] S. Ghosh, V. Sih, W. H. Lau, and D. D. Awschalom, Appl. Phys. Lett. **86**, 232507 (2005).

[26] T. Ozaki, H. Kino, J. Yu, M. J. Han, N. Kobayashi, M. Ohfuti, F. Ishii, T. Ohwaki, H. Weng, M. Toyoda, and K. Terakura: http://www.openmxsquare.org/

[27] R. Dutta and N. Mandal: Appl. Phys. Lett. **101** (2012) 042106.

[28] R. D. King-Smith and D. Vanderbilt: Phys. Rev. B **47** (1993) 1651.

[29] R. Resta: Rev. Mod. Phys. **66,** 889 (1994).

[30] A. Malashevich and D. Vanderbilt: Phys. Rev. B **75,** 045106 (2007).

[31] A. D. Corso, M. Posternak, R. Resta, and A. Baldareschi, Phys. Rev. B **50,** 10715 (1994).

[32] H. Matsui and H. Tabata: J. Appl. Phys. **113,** 183525 (2013).

[33] R. Ghosh, D. Basak, and S. Fujihara: J. Appl. Phys. **96,** 2689 (2004).

[34] P. Pant, J. D. Budai, and J. Narayan: Acta Mater. 58, (2010) 1097.

[35] M. Al-suleiman et al., Appl. Phys. Lett. **91** (2007) 081977.

[36] T. Koga, J. Nitta, H. Takayanagi, and S. Datta, Phys. Rev. Lett. **88**, 126601 (2002).

[37] S. Ghosh, V. Sih, W. H. Lau, and D. D. Awschalom, Appl. Phys. Lett. **86**. 232507 (2005).

[38] Y. Kozuka, S. Teraoka, J. Falson, A. Oiwa, A. Tsukazaki, S. Tarucha, and M. Kawasaki, Phys. Rev. B **87**, 205411 (2013).

[49] H. H. Zhang, et. al., App. Phys. Lett. **104**, 112106 (2014).

[40] P. Schroer, P. Kruger, and J. Pollmann, Phys. Rev. B **49**, 17092 (1994).

[41] P. Ding, et. al., J. Cryst. Growth **331**, 15 (2011).

[42] T. Oguchi and T. Shishidou, J. Phys. Cond. Matt. **21**, 092001 (2009).

[43] E. Simon, et. a, Phys. Rev. B **81**, 235438 (2010).

[44] S. Vajna, et. al., Phys. Rev. B **85**, 075404 (2012).

[45] S. Dohrmann, et. al., Phys. Rev. Lett. **93**, 147405 (2004).

[46] O. D. D. Couto, et. al., Phys. Rev.Lett. **8**, 036603 (2007).

[47] Y. Ohno, et al., Phys. Rev. Lett. **83**, 4196 (1999).

学 位 論 文 審 査 報 告 書 （甲）

１．学位論文題目（外国語の場合は和訳を付けること。）

Density-functional theory based calculations of spin-orbit interaction in ZnO

（ZnO におけるスピン軌道相互作用の密度汎関数理論に基づく計算）

２．論文提出者

(1) 所　　属　　　数物科学　　　　　　専攻

(2) 氏　　名　　MOH. ADHIB ULIL ABSOR

３．審査結果の要旨（600～650字）

7月23日に主査、副査が参加して予備審査を行い、7月30日に学位論文公聴会を行った。公聴会の直後に、主査と副査4名が協議し、合格と判断した。新しいスピントロニクスデバイスを開発する上で、材料がスピン軌道相互作用の影響によりどのような新奇物性を持ちえるのかを明らかにする事が必要である。本研究では、良好な 2 次元電子ガスを生成する酸化亜鉛結晶に着目し、その物性を、量子力学に基づくシミュレーションにより明らかにした。このシミュレーションでは、スピン軌道相互作用を取り入れた電子状態計算を行った。はじめに、結晶に 2 軸応力ひずみが生じたときの計算を行った。その結果、ひずみをかける事により Rashba 効果における Rashba パラメータを制御できる事を明らかにした。とくに、引張応力と圧縮応力の印加では、Rashba 回転の方向が反対となる事が明らかになった。また、応力が結晶内部の電場に影響を与えそれが Rashba パラメータを決める重要な因子となっている事を明らかにした。つぎに、(1010)表面の研究を行った。その結果、ウルツ鉱型結晶材料ではじめて、永続スピンヘリックス構造を持つスピンテクスチャを発見した。スピン寿命が増大する永続スピンヘリックス構造は、これまで閃亜鉛鉱型結晶材料でのみ発見されており、それとは異なる対称性を持つ系で発見した意義は大きい。本研究は、将来のデバイス応用に重要な知見を与える基礎研究であり、本博士論文を合格と判断した。

４．審査結果

(1) 判　　定（いずれかに○印）　　（合 格）・ 不合格

(2) 授与学位　　　博　士（理学）